To appear in Proceedings of the 2008 Asilomar Conference on Signals, Systems, and Computers.

Signal-Domain Registration for Change Detection in Time-Reversal SAR

Nicholas O'Donoughue[1], José M.F. Moura[1] and Yuanwei Jin[2]
[1]Electrical and Computer Engineering
Carnegie Mellon University
Pittsburgh, PA 15213
[2]Engineering and Applied Sciences
Univ. of Maryland, Eastern Shore
Princess Ann, MD 21853

***Abstract*— Change detection is a well-studied area of radar, involving the coherent comparison of two or more images. This is an important tool used to aid in surveillance, battle damage assessment, and other monitoring applications. For many of these applications, registration of the processed SAR imagery is sufficient, as opposed to registration of the raw signal-domain data. Time Reversal SAR, however, is an adaptive waveform transmission technique for SAR that requires coherent processing of the data before image formation algorithms are applied. Change detection for TR-SAR, then, must be performed as a pre-processing step. Ideally, the two change detection data collections would occur over the same trajectory and antenna positions, but this is not practical, and signal registration methods, rather than post-processing image registration, need to be developed and used to compensate for variations in the antenna's positions.**

In this work, we perform registration in the pre-processing stage, i.e., in the signal domain rather than in the image domain. We consider change detection in a mono-static TR-SAR scenario with the SAR antenna mounted on a linear railing, derive a model for the variations in trajectory positions between the two data collections, present our pre-processing methods, and verify them with experimental data.

***Index Terms*— Image Registration, Coherent Processing, Change Detection, SAR, Time-Reversal, TR-SAR**

I. Introduction

Coherent processing schemes, like change detection, are a well studied area of image and radar processing [1], [2]. Historically, research has focused on change detection using post-processing methods, operating on imagery generated with SAR (Synthetic Aperture Radar) algorithms. Recently, Time Reversal SAR [3], [4], [5] has created a need for this comparison to be conducted in the pre-processing stage, using the signal domain data before any image formation algorithms are applied. This is needed to develop an accurate representation of the target channel response, the response of a system induced by the addition of a new target or targets, which is vital for TR-SAR.

There is little prior work focused on registering two SAR data collections in the signal domain, although research to compensate for linear and non-linear motion of the TR-SAR antenna along the trajectory is relatively well known [6], [7], [8], [9]. The majority of motion compensation research focuses on known motion artifacts, usually collected from an onboard GPS and accelerometer [1], [2], [10], [11]. We assume no such knowledge, and the work presented here can be thought of as compensation for unknown motion.

In this work, we will first discuss the necessary background information and further explanation of the need for signal domain registration in Section II, then define the SAR system model and assumptions made concerning the position error between two data collections in Section III. Section IV details the analysis of the position error as well as the proposed method for compensation. Experimental results are reported in Section V, and the conclusion is given in Section VI.

II. Background

Time Reversal SAR [3], [4], [5], [12] is an adaptive waveform transmission technique recently developed to optimize signal-to-noise ratio (SNR) and detection probability. This technique is beneficial for systems deployed in highly cluttered environments, where the multi-path response is significant. In Time Reversal (TR) systems [13], [14], there is usually a two-stage transmission phase consisting of 1) a probing signal, and 2) the TR probing signal. This is sometimes referred to as Physical Time Reversal. Mathematical Time Reversal is an alternative to physical retransmission that is used in the processing stage.

Change detection is a process for discovering any differences in a scene between two measurements, which we refer to as the calibration step and the detection step. It is necessary for the two measurements to be aligned for change detection processing, thus registration is used. In conventional SAR, registration can be done in the image domain data (post-processing), but in TR-SAR the change detection and registration must both occur in the signal domain (pre-processing). This is because TR-SAR utilizes the result, which we refer to as the target channel response, as an input to the TR probing signal.

In [3], [4], [5], [12], [13], the target channel response is obtained by direct subtraction of the probing signal response during the detection step (step 2) and the signal response at some earlier calibration step (step 1), when the target is known not to be present. This direct subtraction approach is justified because of the intractable nature of estimating the multi-path components of the target channel response in highly-cluttered environments. But, this approach requires perfectly repeatable antenna positions, as the two response matrices must align

This work is partially funded by the Defence Advanced Research Projects Agency through the Army Research Office under grant no. W911NF-04-1-0031.

Fig. 1. Rail-SAR System at RMS, Tucson, AZ

perfectly for subtraction. In other words, each pulse in the detection step must be transmitted and measured at the exact same position as the corresponding pulse in the calibration step. In this paper, we formulate a registration technique for raw TR-SAR data, which will account for a uniform offset in the antenna array positions. The reasons for assuming a uniform offset in the array are discussed in Section III.

A. Possible Applications

We discuss the strengths of TR-SAR, and the applications of the work presented here. TR-SAR can be used as a method for detecting the presence of a target or imaging scenes, specifically in highly cluttered environments. This is because the multi-path response of a dense-clutter environment is used constructively in Time Reversal processing, and is used to increase the performance in situations where traditional SAR suffers artifacts. By exploiting these strengths, we can deploy a time reversal based SAR (TR-SAR) system to monitor a forest or dense urban environment, increasing the probability of detecting a target or changes in the region of interest.

III. Physical Model

For this work, we assume a rail-mounted SAR (RailSAR) system, ≈ 10m in length, elevated 9.2m off the ground plane, using pulse-compressed 'chirp' signals. The region of interest is 442m down range, and is approximately 20m wide (azimuth) by 10m deep (range). The system operates in motion with a PRF (Pulse-Repetition Frequency) of 8Hz, and a track velocity of .06m/s, corresponding to an inter-element spacing in the SAR antenna positions of $\Delta_u = v/PRF = \frac{3}{4}$cm. These are the specifications of a test system deployed at Raytheon Missile Systems, in Tucson, AZ (see figure 1).

In order to perform change detection and TR-SAR, we perform two runs of the RailSAR system (calibration and detection) and compare the data collected. As mentioned before, change detection requires that the pulses line up between the two data measurement steps. Variability in the position of the antenna between data collections is induced by the motor that propels the antenna assembly along the railing, which has an unknown ramp-up acceleration. In other words, the position of the antenna along the track has an initial non-linear stage, where the motor is accelerating to the final velocity of .06m/s (this stage is on the order of $l \leq 1$m), followed by a long linear stage (on the order of $L \approx 9$m). Finally, there is a small, possibly variable, amount of time at the end of the array where the motor has stopped, but the antenna continues to take measurements, resulting in an unknown number of repeated pulses at the end of the array.

To resolve this variability, we pre-process the data as follows. We first ignore the leading 120 pulses (corresponding to 1m of rail) to remove the initial non-linear stage, and retain only 1200 pulses (corresponding to 9m of rail) to remove the trailing repeated pulses. This is done so that the datasets we are working with correspond to uniformly sampled arrays. This cropping of pulses results in a slight loss of resolution in the system, since we are reducing the size of the synthetic aperture. We work with a uniformly sampled array. This avoids distortion in both imaging of the scene and registration of the datasets. Non-uniformly sampled arrays can only be used if the sample spacing is accurately known, as SAR image formation algorithms require coherent processing of the data samples at each antenna position. Working with uniformly sampled arrays, the two datasets obtained can now be considered collections from the same exact trajectory, except for an unknown uniform translation (Δ_x), see figure 2.

A. Generalization

In general, if we were to consider an aircraft attempting to follow the same trajectory in both data collections, the variations in antenna positions between the calibration and detection steps of change detection would need to be modeled using three translational error terms $(\Delta_x, \Delta_y, \Delta_z)$ as well as three rotational error terms $(\theta_{xy}, \theta_{xz}, \theta_{yz})$. These six error quantities should be considered random variables that vary over the duration of the synthetic array. Since our system is confined to a fixed railing, we can ignore all of the rotational terms, and two of the three translational terms as a first approach. Furthermore, we have made the assumption that the remaining translational term Δ_x has no variation, it is uniform across the array. This simplification is justified; it corresponds to modeling our dataset as the linear stage of the motor's operation.

IV. Method

A. Change Detection Problem Statement

We are attempting to register two sets of SAR data by compensating for the differences in antenna positions caused by the variable ramp-up time for the railSAR motor. The first set of data, $s_c\left(n, \widehat{t}\right)$, is the measurement taken during the system's calibration step, when the target is known to be absent (we call this 'clutter only'). The second set of data, during the system's detection step, is collected when the target may or may not be present, and the response is $s_d\left(n, \widehat{t}\right)$. Both sets

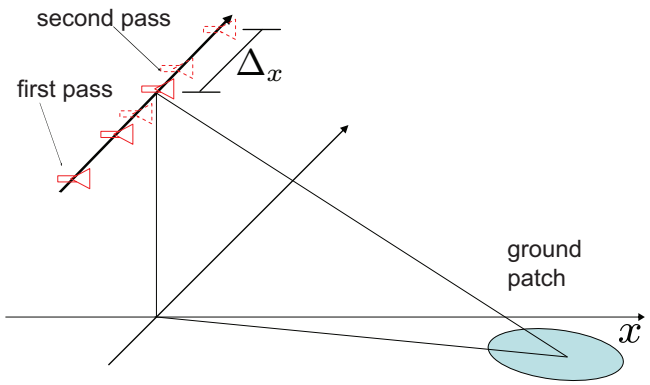

Fig. 2. Linear Array Offset

of data are indexed by the pulse number (n), and the time index relative to the start of each pulse ($\widehat{t}$). Since the data is taken from measurements in a RailSAR system, as described in Section III, we assume that the two trajectories are linear and parallel, both lying in the XZ-plane, at an elevation Z_p above the X-Axis, with a uniform sampling interval. We also assume a uniform translation, Δ_x, between the two arrays (see figure 2).

The array offset can be broken into two parts: a discrete pulse offset (K) and a sub-pulse misalignment (δ_x).

$$\begin{aligned} \Delta_x &= K\Delta_u + \delta_x \\ \text{where } K &\in \mathcal{Z} \\ \text{and } \delta_x &< \Delta_u. \end{aligned} \tag{1}$$

Recall that the quantity Δ_u is the inter-element spacing between pulses along the array, which is $\frac{3}{4}$cm in the RailSAR system.

In order to articulate the effect of δ_x, we analyze the signal equations based on [10]:

$$\begin{aligned} s_c\left(n,\widehat{t}\right) &= \alpha_t e^{-\jmath\frac{4\pi\gamma}{c^2}(R_t-R_0)^2} \\ &\quad e^{-\jmath\frac{4\pi\gamma}{c}\left(\frac{f_c}{\gamma}+\widehat{t}-\frac{2R_0}{c}\right)(R_t-R_0)} \end{aligned} \tag{2}$$

$$\begin{aligned} s_d\left(n,\widehat{t},\delta_x\right) &= \alpha_t e^{-\jmath\frac{4\pi\gamma}{c^2}(R_t+\Delta_R(n,\delta_x)-R_0)^2} \\ &\quad e^{-\jmath\frac{4\pi\gamma}{c}\left(\frac{f_c}{\gamma}+\widehat{t}-\frac{2R_0}{c}\right)(R_t+\Delta_R(n,\delta_x)-R_0)} \end{aligned} \tag{3}$$

We define the variables:

α_t	:	target complex reflectivity
R_t	:	range to the target at pulse n
R_0	:	range to the scene center at pulse n
f_c	:	center frequency
γ	:	chirp rate
T_p	:	pulse length

The quantity $\Delta_R\left(n,\delta_x\right)$ is the change in the range to the target induced by the sub-pulse misalignment, δ_x (note that this range change varies with antenna position $u(n)$), defined as:

$$\Delta_R\left(n,\delta_x\right) = \sqrt{\left(X_c-u(n)-\delta_x\right)^2+Y_c^2+Z_p^2} - R_t(n) \tag{4}$$

The quantity $R_t(n)$ is range to the target:

$$R_t(n) = \sqrt{\left(X_c-u(n)\right)^2+Y_c^2+Z_p^2}. \tag{5}$$

We will approximate this quantity using the 2nd-order Taylor Series approximation $\sqrt{1+x} \approx 1+\frac{1}{2}x$ (which is valid for $x \ll 1$). The approximation takes the form:

$$\begin{aligned} R_t(n) &= \sqrt{Y_c^2+Z_p^2}\sqrt{1+\frac{\left(X_c-u(n)\right)^2}{\left(Y_c^2+Z_p^2\right)}} \\ &\approx \sqrt{Y_c^2+Z_p^2}+\frac{\left(X_c-u(n)\right)^2}{2\sqrt{Y_c^2+Z_p^2}} \end{aligned} \tag{6}$$

We utilize this result, and repeat the Taylor Series approximation to calculate the change in the range to the target:

$$\begin{aligned} \Delta_R\left(n,\delta_x\right) &= \sqrt{Y_c^2+Z_p^2}\sqrt{1+\frac{\left(X_c-u(n)-\delta_x\right)^2}{\left(Y_c^2+Z_p^2\right)}} \\ &\quad -R_t(n) \\ &\approx \sqrt{Y_c^2+Z_p^2}\left(1+\frac{\left(X_c-u(n)-\delta_x\right)^2}{2\left(Y_c^2+Z_p^2\right)}\right) \\ &\quad -R_t(n) \\ &\approx \sqrt{Y_c^2+Z_p^2}+\frac{\left(X_c-u(n)-\delta_x\right)^2}{2\sqrt{Y_c^2+Z_p^2}} \\ &\quad -R_t(n) \\ &\approx R_t(n)+\frac{\delta_x^2-2\delta_x\left(X_c-u(n)\right)}{2\sqrt{Y_c^2+Z_p^2}} \\ &\quad -R_t(n) \\ &\approx \frac{\delta_x^2-2\delta_x\left(X_c-u(n)\right)}{2\sqrt{Y_c^2+Z_p^2}} \end{aligned} \tag{7}$$

B. Solution

We separate Δ_x into two components in order to isolate its effects on the received signal. The pulse offset (K) is a simple translation and has no effect on the form of the received signal, only effecting the location of that pulse in the data matrix. The sub-pulse misalignment (δ_x), however, has two distinct effects. This slight change in position causes a change in the distance from the antenna to the target. The change in range to the target impacts the phase of the received signal and, if the sampling interval is fast enough, can induce a time delay in receiving the signal, referred to here as τ. We take a two-step approach to compensate for the effects of K and δ_x: 1) Pulse Correlation corrects the pulse offset (K) and time delay (τ), and 2) Sub-Pulse Registration corrects the phase effects.

Pulse Correlation. The first step in registering the two SAR datasets is to align the corresponding pulses and correct time delay. We assume that the normalized 2-D cross-correlation of

the two datasets provides adequate registration of the integer pulse offset, K, and induced time delay τ. This is reasonable because cross-correlation is the optimal approach to aligning the signals, in an MMSE sense, when the signal noise is Gaussian.

To register the images for K and τ, but before we correct for the phase effects induced by δ_x, we cross-correlate the magnitued images, i.e.,

$$\widetilde{K}, \widetilde{\tau} = \arg\max \frac{1}{N_K N_\tau} \sum_{n,\widehat{t}} \left| s_c\left(n, \widehat{t}\right) \right| \left| s_d\left(n-K, \widehat{t}-\tau\right) \right| \tag{8}$$

where $N_K N_\tau$ is the number of overlapping elements at pulse shift K and time shift τ. For large datasets, we compute the cross-correlation as a conjugate multiplication in the frequency domain, known as phase correlation.

Sub-Pulse Registration. Once pulse correlation has determined K and τ, we turn to the phase effects in order to correct the sub-pulse misalignment (δ_x). These phase effects can be related to the misalignment δ_x with the equation:

$$\begin{aligned} \Phi\left(n, \widehat{t}, \delta_x\right) &= \angle s_d\left(n, \widehat{t}, \delta_x\right) - \angle s_c\left(n, \widehat{t}\right) && (9) \\ &= \frac{4\pi\gamma}{c^2} \Delta_R^2\left(n, \delta_x\right) \\ &- \frac{4\pi\gamma}{c}\left(\frac{f_c}{\gamma} + \widehat{t} - \frac{2R_t(n)}{c}\right) \Delta_R\left(n, \delta_x\right), && (10) \end{aligned}$$

where $\angle f(x)$ is the phase of $f(x)$.

We perform a non-linear optimization on the SSD (sum of squared difference) of the two pulse-registered matrices, compensating for the phase difference in the second dataset. The optimization metric is given by:

$$\Psi\left(\delta_x\right) = \sum_{n,\widehat{t}} \left| s_c\left(n, \widehat{t}\right) - \widetilde{s}_{t+c}\left(n, \widehat{t}\right) e^{-\jmath\Phi\left(n, \widehat{t}, \delta_x\right)} \right|^2 \tag{11}$$

$$\text{where} \quad : \quad \widetilde{s}_{t+c}\left(n, \widehat{t}\right) = s_d\left(n - \widetilde{K}, \widehat{t} - \widetilde{\tau}\right) \tag{12}$$

$$\text{subject to} \quad : \quad |\delta_x| < \Delta_u. \tag{13}$$

This leads to the optimization function:

$$\widetilde{\delta_x} = \arg\min\left\{\Psi\left(\delta_x\right) + \lambda\delta_x^2\right\}. \tag{14}$$

The second term in our optimization function, $\lambda\delta_x^2$ is a regularization term, sometimes called a penalty term, included to encourage smaller offset values.

C. Change Detection

In [3], [13], change detection is computed using the direct subtraction of the two datasets:

$$s_{cd}\left(n, \widehat{t}\right) = s_d\left(n, \widehat{t}\right) - s_c\left(n, \widehat{t}\right). \tag{15}$$

By applying the registration approach here, we modify the change detection approach and present what we call 'registered differencing':

$$\overline{s_{cd}}\left(n, \widehat{t}\right) = s_d\left(n - \widetilde{K}, \widehat{t} - \widetilde{\tau}\right) e^{-\jmath\Phi\left(n, \widehat{t}, \widetilde{\delta_x}\right)} - s_c\left(n, \widehat{t}\right). \tag{16}$$

In verifying this work, we will use both $s_{cd}\left(n, \widehat{t}\right)$ and $\overline{s_{cd}}\left(n, \widehat{t}\right)$ as inputs to a TR-SAR processing algorithm.

Fig. 3. Target Area for Field Tests

V. Results

We used field test data from the RailSAR system at Raytheon Missile Systems, in Tucson, AZ, to verify our registration approach. In the SAR spotlight region of interest, we placed a dense arrangement of PVC pipes and pipe bundles (see figure 3) that serve as background clutter. For the calibration step, we collected the response of this clutter $\left(s_c\left(n, \widehat{t}\right)\right)$. In the detection step, we inserted a single copper pipe in the center of the group of PVC pipes to act as a target, and repeated the process to measure the target-in-clutter response $\left(s_d\left(n, \widehat{t}\right)\right)$. We then computed the direct subtraction ($s_{cd}\left(n, \widehat{t}\right)$, eq. (15)) and the registered difference ($\overline{s_{cd}}\left(n, \widehat{t}\right)$, eq. (16)) of these datasets, as described in Section IV-C.

We then performed TR-SAR processing, as in [4], first with the direct subtraction ($s_{cd}\left(n, \widehat{t}\right)$) and then with the registered differencing ($\overline{s_{cd}}\left(n, \widehat{t}\right)$). Figure 4 shows the results of TR-SAR image formation using the direct subtraction (top) and the registered differencing (bottom). Each image has a pair of lines, which intersect at the image maximum, corresponding to the estimated target position. Azimuth and range cuts of these images, corresponding to the estimated target position, are given in figure 5.

We can see that the double-peaks in the direct subtraction image (an anomalous effect of the array offset) are successfully removed in the registered differencing approach. The range and azimuth cuts confirm that there are two target peaks in the direct subtraction image, while the registered differencing image shows only the one, true peak. The removal of this double peak improves the achieved azimuth resolution from $\approx .8$m to $\approx .55$m. The achieved range resolution in both cases is $\approx .4$m, this is because the scenario used did not experience any time delay (τ).

VI. Conclusion

This paper presents the derivation and implementation of a pre-processing (signal domain) registration for change detection useful for TR-SAR processing, as opposed to post processing (image domain) registration commonly used in

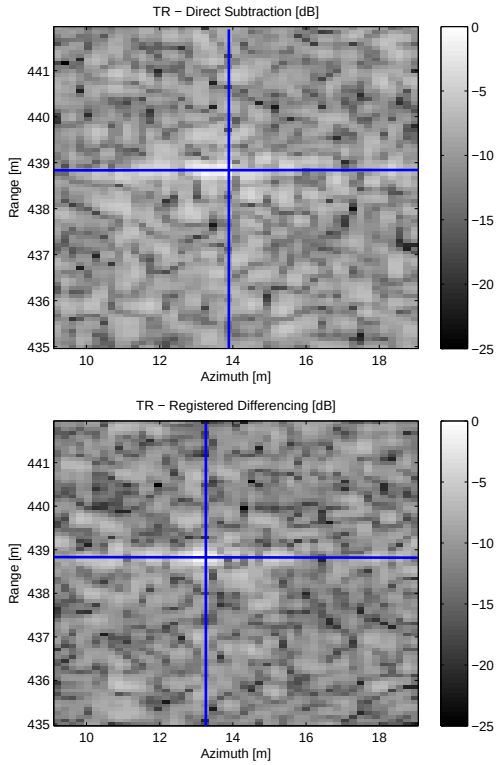

Fig. 4. TR-SAR Change Detection results for experimental data (single target in clutter) processed using direct subtraction (top) and registered differencing (bottom). Cross-hair overlay notes the peak pixel value in each image.

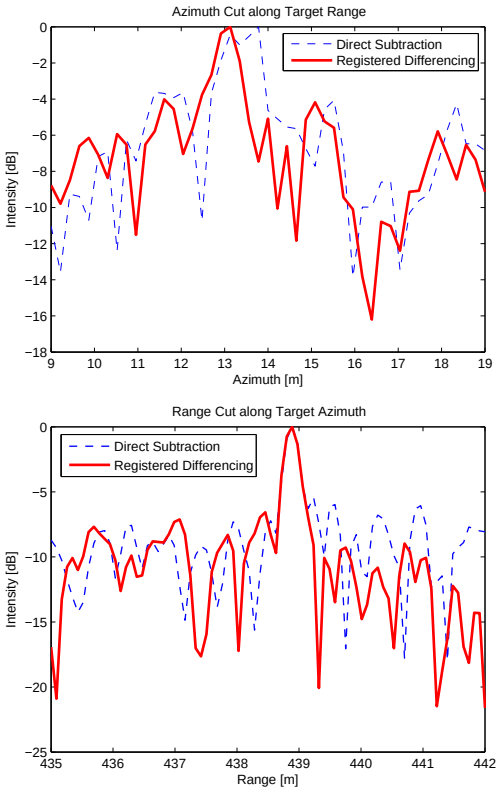

Fig. 5. Range and Azimuth Slices of TR-SAR Change Detection results. Azimuth cuts (top) correspond to horizontal lines in figure 4, range cuts (bottom) correspond to vertical lines in figure 4.

conventional change detection methods. We tested this approach on a rail-mounted SAR system at Raytheon Missile Systems, Tucson, AZ. Experimental data showed that the approach presented here allows change detection in dense scattering environments with TR-SAR.

VII. Acknowledgments

The authors would like to thank Dr. Gustavo Rohde from Carnegie Mellon University for his input, and Raytheon engineers Michael T. Mulford and Laura Santos, who were vital in gathering the experimental data.

Nicholas O'Donoughue is supported by a National Defense Science and Engineering Graduate Fellowship, sponsored by the Army Research Office.

References

[1] M. Soumekh, *Synthetic Aperture Radar Signal Processing*. John Wiley & Sons, Inc., 1999.

[2] P. Tait, *Introduction to Radar Target Recognition*, ser. IEE Radar, Sonar, Navigation and Avionics Series. United Kingdom: The Institution of Electrical Engineers, 2005, vol. 18.

[3] Y. Jin, J. M. F. Moura, N. O'Donoughue, M. Mulford, and A. Samuel, "Time reversal synthetic aperture radar imaging in multipath," in *2007 Asilomar Conference on Signals, Systems, and Computers*. Asilomar, CA: IEEE, Nov 2007.

[4] Y. Jin, J. M. F. Moura, Y. Jiang, J. Zhu, and D. Stancil, "Time reversal target focusing in spotlight SAR," in *15th Adaptive Sensor Array Processing (ASAP) Workshop*. Lexington, MA: MIT Lincoln Lab, June 2007.

[5] Y. Jin and J. M. F. Moura, "TR-SAR: Time reversal target focusing in spotlight SAR," in *ICASSP'07, IEEE Int'l Conf. on Acoustic, Speech and Signal Processing*, vol. 2, Honolulu, HI, April 2007, pp. 957–960.

[6] C. Fuxiang, B. Zheng, and Y. Jianping, "Motion compensation for airborne SAR," in *5th Int'l Conf on Signal Processing (WCCC-ICSP 2000)*, vol. 3, Aug 2000, pp. 1864–1867.

[7] X. Gong and J. Fang, "Analyses and comparisons of some nonlinear Kalman filters in POS for airborne SAR motion compensation," in *2007 Int'l Conf on Mechatronics and Automation (2007 IMCA)*, Aug 2007, pp. 1495–1500.

[8] G. Yongmei, H. Wen, and M. Shiyi, "The geometric distortion correction in SAR motion compensation," in *2001 CIE Int'l Conf on Radar*, Oct 2001, pp. 943–946.

[9] Z. Zhenbo, T. Ziyue, and J. Xingzhou, "Research on bistatic SAR motion compensation," in *2006 CIE Int'l Conf on Radar*, Oct 2006, pp. 1–4.

[10] W. Carrara, R. Goodman, and R. Majewski, *Spotlight Synthetic Aperture Radar: Signal Processing Algorithms*. Artech House, Inc, 1995.

[11] C. Jakowatz, D. Wahl, P. Eichel, D. Ghiglia, and P. Thompson, *Spotlight-Mode Synthetic Aperture Radar: A Signal Processing Approach*. Boston, MA: Kluwer Academic Publishers, 1996.

[12] J. M. F. Moura, Y. Jin, D. Stancil, J.-G. Zhu, A. Cepni, Y. Jiang, and B. Henty, "Single antenna time reversal adaptive interference cancellation," in *ICASSP'05, IEEE Int'l Conf. on Acoustic, Speech, and Signal Processing*, vol. 4, 2005, pp. 1121–1124.

[13] J. M. F. Moura and Y. Jin, "Detection by time reversal: Single antenna," *IEEE Transactions on Signal Processing*, vol. 55, no. 1, pp. 187–201, January 2007.

[14] D. Liu, G. Kang, L. Li, Y. Chen, S. Vasudevan, W. Joines, Q. H. Liu, J. Krolik, and L. Carin, "Electromagnetic Time-Reversal Imaging of a Target in a Cluttered Environment," *IEEE Trans. on Antennas and Propagation*, vol. 53, no. 9, pp. 3058–3066, September 2005.